CPC(HEP & NP), 2010, **34**(9): 1375–1378 Chinese Physics C Vol. 34, No. 9, Sep., 2010

Hadron program at COMPASS*

I. Uman[1] (on behalf of the COMPASS collaboration)

Ludwig-Maximilians-Universität München D-80799, Germany

Abstract The fixed target COMPASS experiment at CERN offers the opportunity to search for exotic mesons and glueball candidates in the light quark sector with unprecedented statistics. Preliminary results from the 2008 data taken with an incoming negative hadron beam (190 GeV/c, mainly pions) on a liquid hydrogen target are presented. New detectors dedicated to hadron beam measurements have been added. These give access to rare neutral and kaonic channels. An amplitude analysis which will allow to fit simultaneously diffractively and/or centrally produced resonances will be described and compared with those used in the CERN WA102 and BNL E852 experiments.

Key words hadron spectroscopy, light meson spectrum, gluonic excitations, exotic mesons, hybrids

PACS 13.25.-k, 13.85.-t, 14.40.Be

1 Introduction

Our present understanding of the light meson spectrum includes the coexistence of light glueballs, hybrids and multiquark states in the same mass range of conventional light $q\bar{q}$ mesons. Different types of reactions are believed to enhance the production mechanism of these states. Candidate hybrid states ($q\bar{q}g$) with exotic quantum numbers, i.e. $\pi(1400)$ and $\pi(1600)$ which cannot be associated to ordinary mesons, were seen as diffractively excited states in the E852 end VES experiments. In addition, $\pi(1400)$ was also seen in proton-antiproton annihilation in the Crystal Barrel experiment and $\pi(1600)$ has been observed recently by COMPASS in 2004 data [1]. The existence of glueballs is still a controversial subject. Glueballs can have indeed the same quantum numbers as conventional mesons, so their evidence must be based mainly on their decay and production properties. If initially glueballs were supposed to decay flavor blind to lightest pseudoscalars nowadays their decay branching fractions are explained within the glueball mixing scheme with conventional mesons and eventually with tetraquarks. The decay branching fractions which are mainly used as a reference for this mixing scheme are calculated using the results of the WA102 experiment at CERN with incoming proton beam at 450 GeV on a proton target [2].

The mechanism of central production observed by the WA102 experiment is believed to be Double Pomeron Exchange (DPE). With incoming hadron energies of 190 GeV both diffractive and central production are observed, therefore COMPASS can access and confirm with much higher statistics the results of both E852 and WA102 experiment.

Preliminary results of the reconstruction of exclusive, $\pi^-p \to \pi^-\eta\eta p$ and $\pi^-p \to \pi^-K_sK_sp$ final states with 2008 data will be discussed.

2 Detector description

The COMPASS experiment is a two stage detector with a large angle spectrometer area (LAS) for low energetic produced particles and a small angle spectrometer area (SAS) which covers the medium and high energy range. It is located at the CERN Super Proton Syncroton (SPS) which provides high intensity beams, 4×10^7 s^{-1} muons and 5×10^6 s^{-1} hadrons, with momenta up to 300 GeV/c. In the LAS area we have a magnet with a bending power of 1 Tm (SM1), a tracking system, a RICH (Ring Imaging Cerenkov) detector, 1500 channel electromagnetic calorimeter (ECAL1) and a hadronic calorimeter (HCAL1). In the SAS area we have a higher bending power magnet of 4.4 Tm (SM2) with an additional tracking system, a second 3068 channel electromagnetic calorimeter

Received 19 January 2010

∗ Supported by German Bundesministerium für Bildung und Forschung

1) E-mail: ismail.uman@cern.ch

(ECAL2) and a second hadronic (HCAL2) calorimeter. At 190 GeV the incoming negative beam consists mainly of π(93%), K(2.5%), μ(3%), $\bar{p}$(0.6%) and e^-(0.1%) while at incoming positive beam it consists mainly of protons and pions. To identify the incoming beam particles two Cerenkov differential counters with acromatic ring focus (CEDAR) are placed upstream in the beam line. To improve the exclusivity the 40 cm long liquid hydrogen target is surrounded by two concentric rings of scintillators (RPD) which are used to identify recoiling protons by TOF and dE/dx measurements. The performance of ECAL2 has been improved with respect to the pilot run in 2004 by replacing the central lead glass cells with 900 radiation-hard Shashlyk blocks. In addition LASER and LED monitoring system for ECAL2 and ECAL1, respectively, were implemented in 2008 and 2009.

3 Data Selection

About 42% and 21% of the 2008 DATA were processed to select the neutral channels $\pi^- p \to \pi^- \eta\eta$ and $\pi^- p \to \pi^- K_s K_s p$, respectively.

The η mesons are identified by their decay into two photons and their mass reconstruction which is in agreement with the PDG value [3] as can be seen in Fig. 1. Exclusivity neglecting the recoiling proton, which carries a negligible fraction of the incoming beam energy, is demanded by requesting $180 < E_{\pi^-} + E_{4\gamma} < 200$ GeV. Additional exclusivity taking into account the recoiling proton is demanded requiring that the difference between the angle of the recoiling track in the RPD, assumed to be a proton, with the azimuthal angle of the $\pi^- 4\gamma$ system is in the range between $-0.3 < \phi_{\pi^- 4\gamma} - \phi_p - \pi < 0.3$ rad.

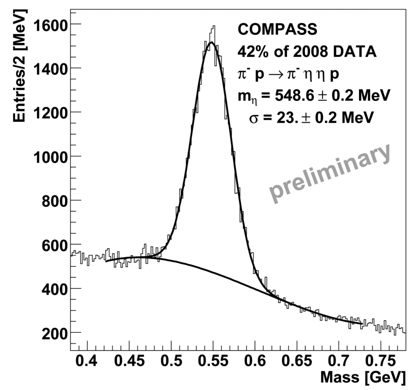

Fig. 1. The two-photon invariant mass for the three possible combinations around the η mass in the $\pi^- p \to \pi^- 4\gamma p$ channel.

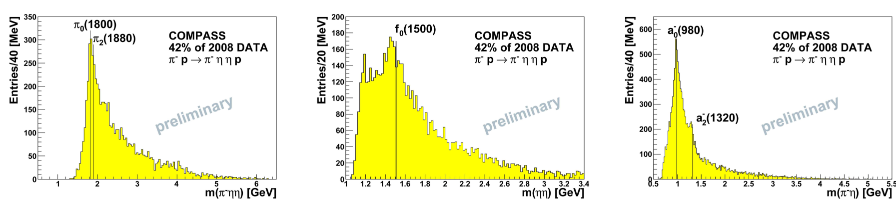

Fig. 2. Invariant mass of the $\pi^-\eta\eta$ (left), ηη (center), and $\pi^-\eta$ (right) systems (not acceptance corrected).

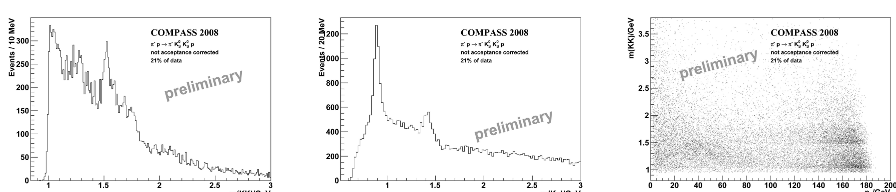

Fig. 3. Invariant mass of the $K_s K_s$ (left), $\pi^- K_s$ (center) and of $K_s K_s$ systems vs. π^- momentum (right).

In the $\pi^-\eta\eta$ mass system a strong peak around 1.8 GeV can be observed (Fig. 2(left)). It is presumably due to the π(1800) but an admixture with π_2(1880) cannot be excluded. In the ηη mass system a structure around 1.5 GeV, which can be associated to the f_0(1500), is visible (Fig. 2(center)).

In the final states $\pi^- p \to \pi^- K_s K_s p$ kaons are identified by their decays into $\pi^+\pi^-$. At high energies K_s travel long distances downstream, which are cut-off by the lack of reconstruction of secondary vertices before SM1 at about 2.5 m. The $K_s K_s$ mass system (Fig. 3(left)) shows similar features around 1.5 GeV which are presumably due to both f_0(1500) and f'_2(1525).

4 Amplitude analysis

Whilst for the 2004 data the partial wave analysis (PWA) was performed using a program which was originally developed at Illinois [4], and later modified at Protvino and Munich [1], for the 2008 data two more independent formalism will be used. One using a PWA program developed at Brookhaven [5] and adapted for COMPASS and another one developed for the $\bar{p}p$ Crystal Barrel experiment at CERN [6] and for the E835 Fermilab experiment at Fermilab [7]. A description and adaptation of the latter formalism for COMPASS will be given here.

From Fig. 3(right) where the mass of the K_sK_s system is plotted vs. the π^- momentum one can see that the enhancement at 1.5 GeV in the K_sK_s invariant mass is pronounced at high π^- momenta, i.e. high pion x_F. This indicates that the $f_0(1500)/f_2'(1525)$ is presumably produced centrally and not as a decay product of a diffractively produced $\pi^-K_sK_s$ system. Indeed because of momentum conservation a central rapidity of the two-body K_sK_s system corresponds to a higher x_F momentum of the scattered π^-. On the other hand, the presence of resonances in the other invariant mass combinations (Fig. 2(right) and 3(center)) indicates that at 190 GeV diffractive excitation coexist with central production. This implies that in the amplitude Ansatz two terms have to be fitted, one for each of the production mechanisms. In order to reproduce the average kinematics of these two possible processes, MC simulations have been performed. For a centrally produced resonance X decaying to $\eta\eta$ (Fig. 4) a rapidity y_{cm} of X homogeneously distributed between -1 and 1 in the c.m. frame is assumed. The four-momentum transfer t at each vertex, t_{π^-} to the leading π^- and t_p to the recoiling p is randomized as for the case of two independent elastic vertices, i.e. as e^{-bt}, where b is a typical value of $\sim 6\ \mathrm{GeV}^{-2}$.

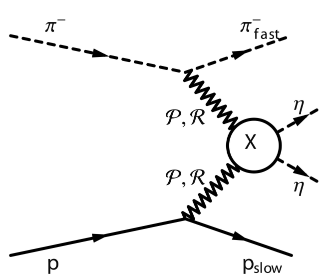

Fig. 4. Feynmann diagram of a central production. $\mathcal{P}$ and $\mathcal{R}$ are exchanged Pomeron or Reggeon.

From Ref. [8]

$$M_X^2 = -x_{P_1} x_{P_2} s, \tag{1}$$

where $x_{P_2} = 1 - x_\pi$ is the momentum fraction in the c.m of the Pomeron emitted by the π, $x_{P_1} = x_p - 1$ is that of the Pomeron emitted by the p and s is the πp c.m. squared energy. In the center of mass

$$x_p + x_\pi + x_X = 0 \tag{2}$$

and

$$x_X = M_T \frac{e^{y_{cm}} - e^{-y_{cm}}}{\sqrt{s}} = \frac{2M_T \sinh y_{cm}}{\sqrt{s}}, \tag{3}$$

where

$$M_T = \sqrt{M_X^2 + p_T}$$

is the transverse mass of the central X. Using Eqs. (1), (2) and (3), the simulations of the x_F of the recoiling proton, fast π^- and central system X have distributions typical for a central production (Fig. 5).

In the case of a diffractively produced state Y with the subsequent decay into π^-X and $X \to \eta\eta$ (Fig. 6) we assume:

$$1 - x_Y = \frac{M_Y^2 - m_{\pi^-}^2}{s}.$$

With the approximation $p_{T,Y}^2 = -t$ the x_F distribution (Fig. 7) of the X system has on average higher values with respect to the one relative to a centrally produced X system (Fig. 5). At 190 GeV energy of the incoming beam the two distribution partly overlap, therefore it is not possible to separate these two different reactions.

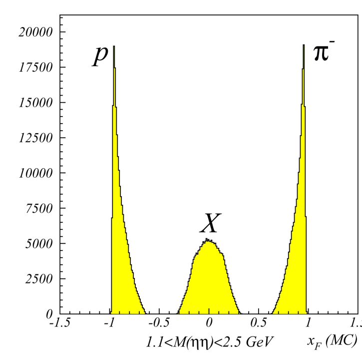

Fig. 5. Generated x_F distributions for a reaction $\pi^-p \to \pi^-Xp$ with a centrally produced resonance $X \to \eta\eta$.

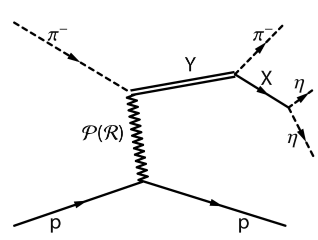

Fig. 6. Feynmann diagram of a diffractive production.

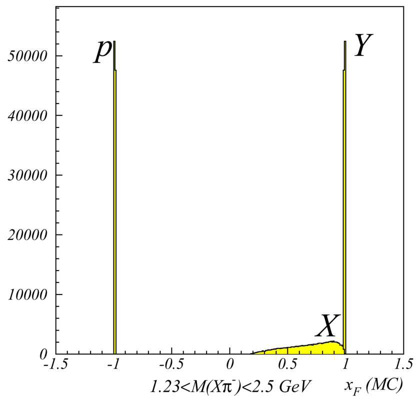

Fig. 7. Generated x_F distributions for a reaction $\pi^- p \to Yp$ with a diffractively produced resonance $Y \to \pi^- X$, with $X \to \eta\eta$.

The decay amplitude is written in terms of relativistic Breit-Wigner functions for the dynamical part and spherical harmonics for the angular part as follows:

$$A_J^\lambda = G_\lambda e^{i\delta_\lambda} F_J(q) \frac{Y_J^\lambda(\alpha,\beta)}{m_0^2 - s - i m_0 \Gamma(m)}.$$

Here λ is the component of the spin along the quantization axis, G_λ and δ_λ are the coupling constant and phase, $F_J(q)$ are the standard centrifugal barrier factors. A sequence of rotations of the reference frame from the beam axis, called Wick rotations, by ϕ and θ relative to the direction of flight of X and a Lorentz boost to the rest system of X and by $-\theta, -\phi$ cancel the D functions which would otherwise be needed for the first rotations. The spherical harmonic $Y_J^\lambda(\alpha,\beta)$ are calculated in this reference frame, with the angles α, β defined by the direction of one of the decay products of the resonance X with respect to the beam direction and production plane. The intensity of two resonances with masses m_0 and m_1, spin J and J′ is given by

$$w(m_0,m_1) = \sum_\lambda [|A^\lambda_{X_J}(m_0)|^2 + |A^\lambda_{Y_{J'}}(m_1)|^2 + 2c_\lambda \mathcal{R}(A^\lambda_{X_J}(m_0) A^{\lambda*}_{Y_{J'}}(m_1)],$$

where $-1 \leqslant c_\lambda \leqslant 1$ is the degree of coherence. The total intensity is fitted minimizing the negative log-likelihood:

$$-\ln\mathcal{L} = -\sum_{j=1}^N \ln(w_j) + N\ln\left(\sum_{i=1}^M w_i\right)$$

with N the number of data events, M the number of MC events, and G_λ, δ_λ, c_λ are the free parameters of the fit. While unknown resonance parameters and quantum numbers are allowed to vary and are optimized in second stage, the masses and widths of well established resonanced are kept fixed at PDG values.

The main differences between this formalism and the standard PWA formalism used in the BNL E852 and WA102 experiments is in the additional degree of coherence which is taking into account, not only the incoherence between natural and unnatural parity exchanges in the reflectivity basis but also the possibility of a partial coherence. In addition, the data are fitted minimizing mass dependent unbinned log-likelihood. This technique should reduce the number of non-mathematical ambiguities observed in standard PWA where the waves are extracted with looser constraints after mass independent binned log-likelihood method. In order to fit the two possible reaction types the MC will include fitted amounts of events with both production mechanisms in order to cover the full phase space of the decaying particles and to reproduce the shape of the x_F and t distributions.

5 Conclusion

After the analysis of 2004 data COMPASS started the reconstruction of high statistics data in several charged and neutral channels with incoming hadron beam at 190 GeV. Preliminary invariant mass distributions show the presence of resonances which are non $\bar{q}q$ candidates. To analyze these data two different formalisms have been developed. The amplitude analyses using these formalisms are in progress.

References

1 Aleeksev M et al (COMPASS collaboration). Submitted to Physical Review Letters. [arXiv:hep-ex/0910.5842v1]

2 Barberis D et al (WA102 collaboration). Phys. Lett. B, 2000, **479**: 59. [arXiv:hep-ex/0003033]

3 Amsler C et al (Particle Data Group). Phys. Lett. B, 2008, **667**: 1

4 Ascoli G, Brockway D V, Crawley H B, Eisenstein B I, Hanft R W, Ioffredo M L, Kruse U E. Phys. Rev. Lett., 1970, **25**: 962

5 Cummings J P, Weygand D P. Report BNL-64637, Brookhaven National Laboratory (1997)

6 Amsler C et al (Crystal Barrel collaboration). Phys. Lett. B, 2006, **639**: 165

7 Uman I, Joffe D, Metreveli Z, Seth K K, Tomaradze A, Zweber P. Phys. Rev. D, 2006, **73**: 052009. [arXiv:hep-ex/0607034]

8 Faessler M, Geyer R. 7.5.06 COMPASS note 2006-7